

## Molecular modeling of the structure and dynamics of the interlayer and surface species of mixed-metal layered hydroxides: Chloride and water in hydrocalumite (Friedel's salt)

ANDREY G. KALINICHEV,<sup>1,\*</sup> R. JAMES KIRKPATRICK,<sup>1</sup> AND RANDALL T. CYGAN<sup>2</sup>

<sup>1</sup>Department of Geology, University of Illinois at Urbana-Champaign, 1301 W. Green Street, Urbana, Illinois 61801, U.S.A.

<sup>2</sup>Geochemistry Department, Sandia National Laboratories, Albuquerque, New Mexico 87185-0750, U.S.A.

### ABSTRACT

The dynamical behavior of Cl<sup>-</sup> and H<sub>2</sub>O molecules in the interlayer and on the (001) surface of the Ca-aluminate hydrate hydrocalumite (Friedel's salt) over a range of temperatures from -100 to 300 °C was studied using isothermal-isobaric molecular dynamics computer simulations. This phase is currently the best available model compound for other, typically more disordered, mixed-metal layered hydroxides. The computed crystallographic parameters and density are in good agreement with available X-ray diffraction data and the force field developed for these simulations preserves the structure and density to within less than 2% of their measured values. In contrast to the highly ordered arrangement of the interlayer water molecules interpreted from the X-ray data, the simulations reveal significant dynamic disorder in water orientations. At all simulated temperatures, the interlayer water molecules undergo rapid librations (hindered hopping rotations) around an axis essentially perpendicular to the layers. This results in breaking and reformation of hydrogen bonds with the neighboring Cl<sup>-</sup> anions and in a time-averaged nearly uniaxial symmetry at Cl<sup>-</sup>, in good agreement with recent <sup>35</sup>Cl NMR measurements. Power spectra of translational, librational, and vibrational motions of interlayer and surface Cl<sup>-</sup> and H<sub>2</sub>O were calculated as Fourier transforms of the atomic velocity autocorrelation functions and compared with the corresponding spectra and dynamics for a bulk aqueous solution. The ordered interlayer space has significant effects on the motions. Strong electrostatic attraction between interlayer water molecules and Ca atoms in the principal layer makes the Ca...OH<sub>2</sub> bond direction the preferred axis for interlayer water librations. The calculated diffusion coefficient of Cl<sup>-</sup> as an outer-sphere surface complex is almost three times that of inner-sphere Cl<sup>-</sup>, but is still about an order of magnitude less than that of Cl<sup>-</sup> in bulk aqueous solution at the same temperature.

### INTRODUCTION

Mixed-metal layered hydroxides (MMLHs), also called layered double hydroxides (LDHs) and "anionic clays," are among the few oxide-based materials with permanent anion exchange capacity developed through isomorphous substitution. They occur in many natural environments, are readily synthesized, and are receiving rapidly increasing attention for a wide variety of applications in catalysis, environmental remediation, and medicine (e.g., Ulbarri et al. 1995; Newman and Jones 1998, Schmassmann et al. 1993). They also play a key role in cement chemistry, due to their importance in controlling the chemical behavior of anionic species (Taylor 1997). MMLHs have a layered structure typically based on that of brucite or portlandite. Substitution of 3+ cations (often Al) for 2+ cations (often Mg or Ca) in the principal hydroxide layer leads to a permanent positive charge. This charge is compensated by anions, which have associated water molecules, in the interlayer space and on the particle surfaces.

Hydrocalumite, [Ca<sub>2</sub>Al(OH)<sub>6</sub>]Cl·2H<sub>2</sub>O, also known as Friedel's salt, is unique among MMLHs, because it has not only an ordered Ca-Al distribution in the hydroxide layer, but well ordered Cl<sup>-</sup> and water in the interlayer space. The interlayer order is due to coordination of the water molecules to Ca in the hydroxide layer, which results in an unusual sevenfold-coordinated Ca environment. This phase occurs naturally (Fischer et al. 1980; Passaglia and Sacerdoti 1988; Sacerdoti and Passaglia 1988) and also forms by reaction of Cl-containing deicing salts with the calcium aluminates of Portland cement (Birnin-Yauri and Glasser 1998).

Because of its structural order and occurrence as relatively large crystals, hydrocalumite is the only MMLH for which a single crystal structure refinement is available (Terzis et al. 1987). Thus, it is currently the best model compound for understanding the structure and dynamical behavior of surface and interlayer water and anions in MMLHs. Such understanding is essential for exploitation of the unique anion exchange capabilities of this important class of compounds. Recent <sup>35</sup>Cl NMR spectroscopic study of hydrocalumite in our laboratory is broadly consistent with the structure determined by XRD, but has provided important new insight into the dynamical be-

\*On leave from the Institute of Experimental Mineralogy, Russian Academy of Sciences, Chernogolovka, Moscow Region, 142432, Russia. Current E-mail: audreyk@hercules.geology.uiuc.edu

havior of surface and interlayer  $\text{Cl}^-$  and has identified a previously unknown dynamical phase transition at 6 °C (Kirkpatrick et al. 1999). Below this temperature the  $\text{Cl}^-$  has triaxial symmetry, as expected from a rigid interlayer structure. Above this temperature the  $\text{Cl}^-$  symmetry is uniaxial or nearly so and can only be explained by relative motion (dynamical disorder) of the interlayer species at frequencies greater than about  $10^5$  Hz. Parallel NMR work on the analogous Mg,Al MMLH (a hydroxalcalite-like compound) with  $\text{Cl}^-$  in the interlayer shows that this type of behavior may be common in this group of compounds.

This paper presents the first molecular dynamics (MD) computer simulations of hydrocalumite, with major emphasis on the interlayer structure and the contrasting dynamical behavior of the interlayer and surface species for the time scale from femtoseconds to hundreds of picoseconds. The results also provide a specific structural model for the motion of the interlayer species that causes the uniaxial  $\text{Cl}^-$  symmetry in the high temperature phase and demonstrate the unique capabilities of combined NMR and MD studies to understand the structure and dynamics of surface and interlayer species in water-rock systems.

There has been significant recent effort to model mineral-water interactions by computer simulation. There has been substantial progress in modeling the structure of water and hydrated interlayer cations in smectites (e.g., Chang et al. 1997; Smith 1998; Hartzell et al. 1998). Hydration and dehydration of clays has been simulated in some detail (Delville 1995; Karaborni et al. 1996), and the molecular dynamics of proton binding to mineral oxide surfaces has also been studied (Rustad et al. 1998).

In many of these simulations, however, the atoms of the main oxide layers are treated as fixed in a rigid lattice, except for the degrees of freedom associated with swelling and lateral displacements of the lattice as a whole. This simplified approach saves substantial amounts of computer time and is efficient at providing useful structural information. However, it has inherent and substantial limitations for dynamic modeling of surface and interlayer species. Due to the immobility of the lattice atoms, there is no exchange of momentum and energy between the atoms of the main layers and the interlayer/surface species. Thus, in these models the imposed momentum and energy conservation laws a priori prevent accurate representation of the dynamics of such processes as hydrogen bonding, adsorption, and surface complexation. Surface diffusion rates can be overestimated, and the structure of the water layers at the interface can be distorted. Studies modeling ionic complexes in clays and MMLHs with all atoms in the system movable are beginning to appear in the literature (Aicken et al. 1997; Teppen et al. 1997; Hartzell et al. 1998; Newman et al. 1998; Williams et al. 1999), but to date these concern primarily questions of structure and swelling, and not the dynamics of interlayer and surface species.

The MD simulations reported here realistically model the dynamics of all main layer, interlayer and surface atoms on the time scale from  $10^{-15}$  to  $10^{-10}$  s and are specifically aimed at probing the dynamic behavior of the interlayer and surface anions.

## SIMULATION METHODS

The initial hydrocalumite structure for our simulations was taken from the X-ray diffraction results of Terzis et al. (1987), which has monoclinic  $C2/c$  symmetry. The MD simulation cell contains  $2 \times 2 \times 1$  crystallographic unit cells in the  $a$ ,  $b$ , and  $c$  directions, respectively. Except for the three dimensional periodic boundary conditions (e.g., Allen and Tildesley 1987) imposed on the simulation supercell, there were no additional symmetry constraints. The structure was treated as triclinic, and all cell parameters,  $a$ ,  $b$ ,  $c$ ,  $\alpha$ ,  $\beta$ ,  $\gamma$ , were considered independent variables during the isothermal-isobaric MD simulations.

The total potential interaction energy of the simulated system consisted of a Coulombic term for all electrostatic interactions between partial atomic charges and a Lennard-Jones (12-6) term modeling the van-der-Waals dispersive interactions:

$$U = \sum_{i,j} \left\{ \frac{q_i q_j}{4\pi\epsilon_0 r_{ij}} + 4\epsilon_{ij} \left[ \left( \frac{\sigma_{ij}}{r_{ij}} \right)^{12} - \left( \frac{\sigma_{ij}}{r_{ij}} \right)^6 \right] \right\} \quad (1)$$

where  $r_{ij}$  is the distance between atoms  $i$  and  $j$ ,  $q_i$ ,  $q_j$  are partial charges centered on these atoms,  $\epsilon_{ij}$  and  $\sigma_{ij}$  are parameters of the Lennard-Jones interaction potential, and  $\epsilon_0$  is the dielectric permittivity of vacuum ( $\epsilon_0 = 8.85419 \times 10^{-12}$  F/m). The interaction parameters from the augmented ionic consistent valence force field (CVFF) within the Cerius<sup>2</sup> molecular modeling package (Molecular Simulations Inc. 1998) were used as a basis for construction of a force field to model all ion-ion and ion-water interactions in our simulations. However, the original force field was modified in several significant aspects.

For water-water interactions we used the flexible version of the simple point charge (SPC) interaction potential (Berendsen et al. 1981) as developed by Teleman et al. (1987). Lennard-Jones terms centered on the O atoms were assumed equivalent for both  $\text{H}_2\text{O}$  and OH-group O atoms, while those centered on the H atoms were ignored. The harmonic potential of the hydroxide OH-group stretching vibrations was also taken equivalent to that of  $\text{H}_2\text{O}$ .

Instead of placing full formal charges on the metal ions, we performed preliminary quantum-mechanical calculations to develop appropriate partial charges. The electronic structure of hydrocalumite was determined using periodic density functional theory (DFT) as implemented with the Dmol3 program (Delley 1990). Heavy atom positions were those reported by Terzis et al. (1987). Appropriate positions for the structural hydrogens in the unit cell were derived by molecular mechanics optimization prior to the DFT calculation. A single point energy calculation was performed for the 88 atoms of the periodic cell that had been converted to P1 symmetry from the original monoclinic space group. Nonlocal corrections were implemented based on the generalized gradient approximation using the Perdew (1991) density functionals for both the electron exchange and correlation. The atomic basis functions included double numeric sets with polarization for all atoms including the hydrogens. A self-consistent field (SCF) and energy convergence (to 0.000001 Ha) were obtained after 20 iterations providing a total energy of  $-1066.066529$  Ha (1 Ha =

2625.5 kJ/mol). A Mulliken analysis of the electron population was performed on the molecular orbitals to obtain the charges of the component atoms.

To make all charges consistent with the chosen water model and the full formal charge of  $-1$  for the  $\text{Cl}^-$  anions, the calculated Mulliken charges on all atoms of the hydroxide layer were scaled up by about 30%. We consider this to be a justifiable procedure, because Mulliken analysis generally underestimates atomic partial charges (Chirlian and Franci 1987; Woods et al. 1990; Teppen et al. 1997). The final set of interaction parameters used in our simulations is presented in Table 1. The Lennard-Jones parameters of unlike interactions were calculated according to the “arithmetic” combining rules:

$$\sigma_{ij} = \frac{\sigma_{ii} + \sigma_{jj}}{2}; \quad \epsilon_{ij} = \sqrt{\epsilon_{ii}\epsilon_{jj}} \quad (2)$$

A “spline cut-off” method was used to treat long range non-Coulomb interactions, and all long-range electrostatic interactions were treated using the Ewald summation method (e.g. Allen and Tildesley 1987).

Molecular dynamics trajectories of all atoms were generated with a time step of 0.001 ps over a period of 100 ps after a preequilibration MD run of approximately the same length under any given conditions. An isothermal-isobaric molecular dynamics algorithm (Parrinello and Rahman 1981) was used in all simulations, and the pressure was set equal to 1 bar. Simulations were performed for bulk crystals at temperatures between  $-100$  and  $500$  °C, for dehydrated crystals at  $100$  °C, and for the interface of hydrocalumite with bulk liquid water. In the latter case the model crystal was initially cleaved in the interlayer along the (001) crystallographic plane; half of the  $\text{Cl}^-$  anions were left on each of the created surfaces, and the simulated periodic system consisted of four hydroxide layers (infinite in the  $a$  and  $b$  directions) interspersed in the  $c$  direction with a layer of water approximately  $20$  Å thick (Fig. 1). This thickness is sufficiently large to effectively exclude direct interaction of one interface with the other. The number of water molecules in this layer was chosen to reproduce the density of bulk liquid water under ambient conditions ( $\sim 1$  g/cm<sup>3</sup>). We have also performed MD simulations for a bulk NaCl aqueous solution with the same set of interaction parameters to compare the dynamics of  $\text{Cl}^-$  anions and  $\text{H}_2\text{O}$  molecules in the interlayer and in the interfacial region of hydrocalumite with the dynamics of the same species in the bulk aqueous solution. Every fourth time step during the simulations was recorded for further analysis. Thus, for every simulation we were able to

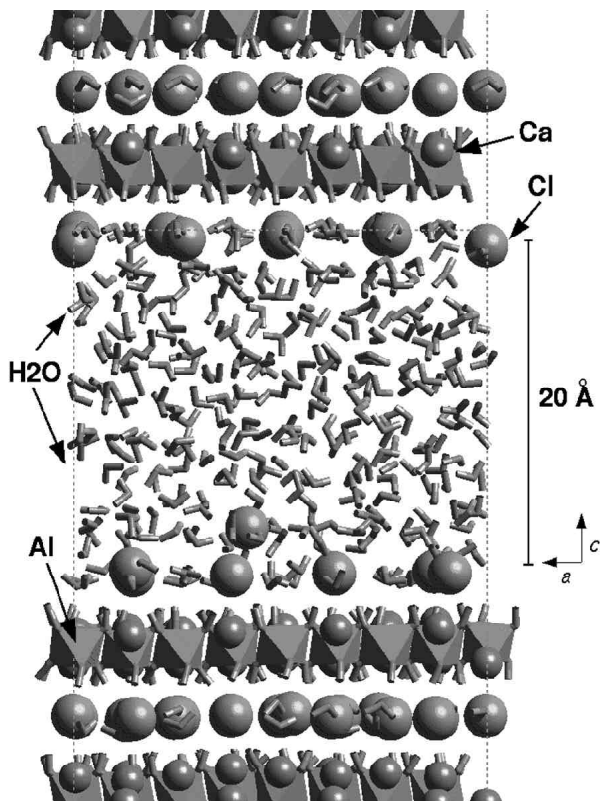


FIGURE 1. A snapshot of the simulation of hydrocalumite/water interface at 25 °C. Octahedra portray Al layers. Small spheres are Ca; larger spheres are Cl.

analyze an equilibrium dynamic trajectory consisting of 25 000 atomic configurations with a time resolution of  $4 \times 10^{-15}$  s. Power spectra of atomic motions in the translational, librational, and vibrational frequency ranges were calculated as Fourier transforms of the velocity autocorrelation functions for each type of atom.

## STRUCTURAL RESULTS

Although all atoms were treated as movable and the size and shape of the simulation cell were not constrained, the structural results demonstrate a remarkable ability of the modified force field to reproduce and preserve the structure and density of the simulated hydrocalumite crystals. The temperature dependencies of all crystallographic unit cell parameters and density are shown in Table 2. The monoclinic angle  $\beta$  and the density are about 2% smaller than in the X-ray results, but all other parameters at room temperature are well within 0.5% of their measured values (Terzis et al. 1987). Angles  $\alpha$  and  $\gamma$  remain within  $0.2^\circ$  of their nominal value of  $90^\circ$ . Statistical uncertainties of the calculated average values in Table 2 were estimated by dividing the total simulated equilibrium MD trajectory into 50 blocks of equal length and calculating individual averages for each block. 95% confidence interval was assumed.

The principal layer consisting of  $\text{Al}(\text{OH})_6$  octahedra distributed in a hexagonal primitive sublattice and connected by Ca atoms is well reproduced and preserved in the MD simulations over the temperature range studied. At room temperature, the

TABLE 1. Parameters of the simulation model

	$\sigma_{ii}$ (Å)	$\epsilon_{ii}$ (kJ/mol)	$q_i$ (e)
<b>Hydroxide layer</b>			
Ca	2.558	5.732	1.6
Al	2.851	0.00188	2.06
O (hydroxide)	3.166	0.650	-1.15
H (hydroxide)	—	—	0.44
<b>Interlayer</b>			
$\text{Cl}^-$	3.981	3.486	-1.0
O (water)	3.166	0.650	-0.82
H (water)	—	—	0.41

**TABLE 2.** Simulated crystallographic lattice parameters and density of hydrocalumite

	Temperature (°C)					
	-100	0	100	200	300	25*
<i>a</i> (Å)	10.000(2)	10.024(2)	10.035(2)	10.053(2)	10.059(2)	9.979(3)
<i>b</i> (Å)	5.770(2)	5.784(2)	5.797(2)	5.803(2)	5.807(2)	5.751(2)
<i>c</i> (Å)	16.28(1)	16.33(1)	16.42(1)	16.55(1)	16.72(1)	16.320(6)
$\alpha$ (°)	89.90(5)	90.07(5)	90.03(5)	90.00(5)	90.16(9)	90.0
$\beta$ (°)	101.95(5)	101.84(5)	101.78(5)	101.76(5)	101.65(5)	104.53(3)
$\gamma$ (°)	89.95(5)	90.01(5)	89.99(5)	89.99(5)	90.00(5)	90.0
<i>V</i> (Å <sup>3</sup> )	919.5(5)	926.5(5)	934.7(7)	945.0(7)	955.5(8)	906.6(4)
<i>r</i> (g/cm <sup>3</sup> )	2.027(1)	2.012(1)	1.994(1)	1.973(1)	1.951(1)	2.056(1)

Notes: Statistical errors in the last significant figure are given in parentheses.

\* Experimental data of Terzis et al. (1987).

average Al-O distance is  $1.92 \pm 0.05$  Å and the average Ca-O distance is  $2.58 \pm 0.05$  Å compared to the experimental values of 1.912 Å and 2.41 Å, respectively (Terzis et al. 1987). The noticeable difference between the calculated and experimental Ca-O distances is largely compensated by some angular distortions of the Ca position in the principal layer, resulting in generally good agreement between the calculated and experimental lattice parameters (Table 2).

According to the X-ray data, the interlayer of composition  $[\text{Cl} \cdot 2\text{H}_2\text{O}]^-$  also consists of a primitive hexagonal sublattice, with  $\text{Cl}^-$  ions forming almost regular triangles of this lattice and water molecules located at the center of each triangle. The orientation of these water molecules is such that each  $\text{Cl}^-$  is coordinated by four H atoms forming ordered chains of hydrogen bonds along the *a* crystallographic direction (Fig. 2a). Each  $\text{Cl}^-$  anion is additionally coordinated by six OH groups (three from two adjacent hydroxide layer). In our simulations these hydrogen bonds keep chlorine virtually immobile even at temperatures as high as 300 °C.

The experimentally observed tenfold-coordinated arrangement of hydrogen bonds to  $\text{Cl}^-$  is well reproduced in our MD simulations. However, in contrast to the highly ordered orientations of the interlayer  $\text{H}_2\text{O}$  molecules interpreted from the X-ray diffraction measurements (Fig. 2a), the simulations reveal significant dynamic disorder in water orientations (Fig. 2b). At all simulated temperatures, the interlayer water molecules undergo librations (hindered hopping rotations) around an axis

essentially perpendicular to the layers. This results in breaking and reformation of hydrogen bonds with the neighboring  $\text{Cl}^-$  anions. At any instant, each water molecule is still hydrogen bonded to 2 chlorides, but because of the hopping among the three possible pairs of chlorides, it is, on average, hydrogen bonded to each one about 2/3 of the time. From the perspective of the  $\text{Cl}^-$  ion, this results in a time-averaged nearly uniaxial symmetry. Although at any instant there are four hydrogen bonds to the neighboring water molecules, averaged over time there are six hydrogen bonds with 2/3 occupancy.

The variable temperature <sup>35</sup>Cl NMR experiments for hydrocalumite (Kirkpatrick et al. 1999) indicate the existence of a dynamical order-disorder phase transition near ~6 °C. Below the transition temperature, the  $\text{Cl}^-$  ion is rigidly held in a triaxial environment, whereas above this temperature, the  $\text{Cl}^-$  is in a dynamically averaged uniaxial environment. The frequency of the atomic motion causing the dynamical averaging which results in the phase transition, must be greater than ~10<sup>5</sup> Hz. Thus, the librational frequencies for water of about 10<sup>13</sup> Hz determined from the present MD simulations (see next section) are much more than sufficient to cause the dynamical averaging observed by NMR.

An interlayer structure with the experimentally observed triaxial  $\text{Cl}^-$  environment is not reproduced in our simulations starting with the high-temperature disordered structure, even at temperatures as low as -100 °C. However, preliminary simulations at still lower temperatures starting from the ordered

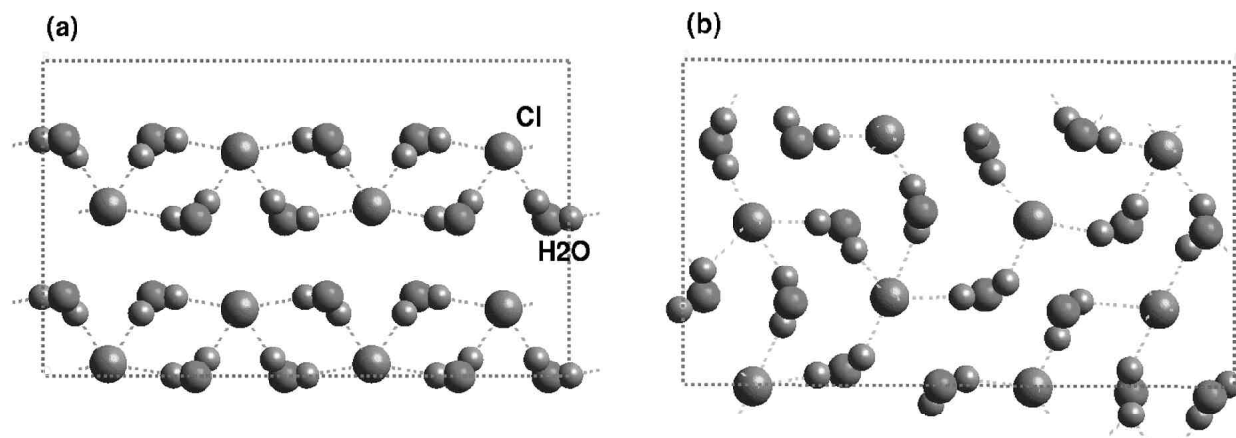


**FIGURE 2.** Interlayer structure of hydrocalumite (view down the *c* direction): (a) ordered structure from the X-ray diffraction data interpretation (Terzis et al. 1987); (b) a snapshot of the orientationally disordered structure resulting from the MD simulations at 0 °C.

structure do indicate the existence of an order-disorder phase transition to a triaxial  $\text{Cl}^-$  environment, change of the space group from  $C2/c$  to  $P2_1/c$ , and an approximately 3% reduction in volume. Detailed analysis of this calculated phase transition and its relationship to the phase transition observed in the NMR experiments (Kirkpatrick et al. 1999) requires more extensive simulations using a larger size of the simulation supercell. These simulations are currently in progress (Kalinichev et al. in preparation).

#### ANION AND WATER DYNAMICS IN HYDROCALUMITE

Power spectra of atomic motions in the translational, librational, and vibrational frequency ranges, calculated as Fourier transforms of the atomic velocity autocorrelation functions, allow comprehensive and detailed analysis of the dynamics in this material. The spectral density of the low frequency vibrational motions of  $\text{Cl}^-$  ions in the interlayer consists of two distinct frequency bands centered at approximately 50 and 150  $\text{cm}^{-1}$  (Fig. 3). Decomposition of chloride velocities into components parallel and perpendicular to the interlayer plane indicates that the 50  $\text{cm}^{-1}$  band is associated with the “in-plane” motions of the anions, and the 150  $\text{cm}^{-1}$  band is associated with the low frequency vibrations perpendicular to this plane. Because each chloride ion is electrostatically bonded to neighboring water molecules and hydroxide groups, these two  $\text{O}\cdots\text{Cl}\cdots\text{O}$  modes of molecular motions are clearly analogous to the intermolecular  $\text{O}\cdots\text{O}\cdots\text{O}$  bending and stretching motions of water molecules in the hydrogen-bonded network, respectively (e.g., Eisenberg and Kauzmann 1969; Heinzinger 1990). Two weaker spectral peaks at  $\sim 110$  and  $\sim 190$   $\text{cm}^{-1}$  are distinctly observable at lower temperatures (Fig. 3c) but merge with the 150  $\text{cm}^{-1}$  peak into one broad spectral band at  $\sim 150$   $\text{cm}^{-1}$  at higher temperatures (Fig. 3a–b). The intensity of the stretching peak is greatly reduced for  $\text{Cl}^-$  ions on the surface of hydrocalumite, where the shape of the  $\text{Cl}^-$  low frequency vibrational spectrum more closely resembles the spectrum in a bulk aqueous solution (Fig. 3b). In the collapsed, dehydrated hydrocalumite structure at high temperature, low frequency vibrations in the plane of the interlayer are the only possible chloride motions, as shown by the very intense peak at  $\sim 50$   $\text{cm}^{-1}$  in Figure 3a.

As for  $\text{Cl}^-$ , the low frequency vibrational dynamics of interlayer water in hydrocalumite is also very different from that of surface water molecules, which is in turn much closer to that of water molecules in the bulk solution (Fig. 4). The main differences are in the frequency range below  $\sim 50$   $\text{cm}^{-1}$ . In particular, there are very low spectral intensities at  $\nu = 0$  for translational motions for surface, and especially interlayer species, compared to the corresponding intensities for the same species in the bulk (Figs. 3b and 4b). This result clearly indicates drastically reduced diffusion coefficients for these species. The shape of the low frequency vibrational spectrum for interlayer water molecules is also strongly correlated with the spectrum of Ca atoms in the main hydroxide layer, because each water molecule is quite strongly electrostatically bonded to a Ca atom. Thus, as proposed in the X-ray structure (Terzis et al. 1987), interlayer water molecules complete the seven-fold-coordinated environment of Ca in the hydroxide layer (Fig. 5),

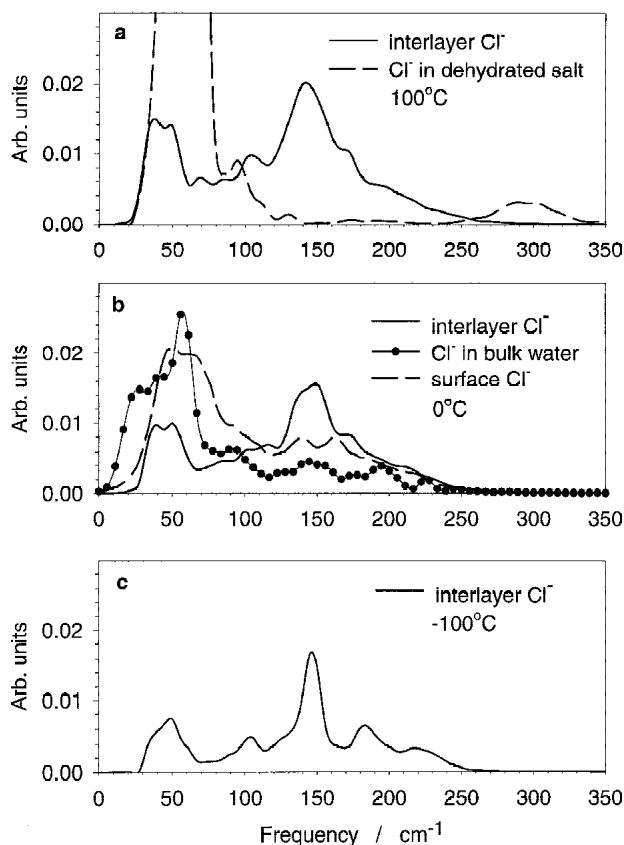


FIGURE 3. Spectral density of the interlayer  $\text{Cl}^-$  low frequency vibrational motions.

with average  $\text{Ca}\cdots\text{O}(w)$  distances essentially equal to those of  $\text{Ca}\cdots\text{O}$  in the main layer ( $\sim 2.57$  Å in our simulations).

The strong electrostatic attraction between the negatively charged oxygen atoms of interlayer  $\text{H}_2\text{O}$  molecules and positively charged Ca atoms in the hydroxide layer makes the  $\text{Ca}\cdots\text{O}(w)$  bond direction the preferred axis for  $\text{H}_2\text{O}$  librations (hindered rotations, Fig. 6). Decomposition of instantaneous velocities of H atoms in water into components parallel and perpendicular to the (001) plane clearly demonstrated that most of the spectral intensity of atomic motions in the librational range of frequencies (around 500  $\text{cm}^{-1}$ ) is associated with an axis parallel to the direction of  $\text{Ca}\cdots\text{O}(w)$  bonds. This is in sharp contrast to the molecular librations in bulk liquid water in which, on average, four equally strong hydrogen bonds act on every water molecule to create almost isotropic librational environment. The result is much broader spectral peaks of these hindered rotations in water (e.g., Heinzinger 1990; Kalinichev and Heinzinger 1992). To some extent, this is also true for the  $\text{H}_2\text{O}$  molecules in the first adsorbed layer on the crystal-water interface (dashed line in Fig. 6b). The calculated spectral bands of intramolecular bending and stretching vibrations of the interlayer  $\text{H}_2\text{O}$  molecules (not shown) are also much narrower in comparison to the corresponding bands in bulk liquid water and shifted to higher frequencies, indicating significantly dif-

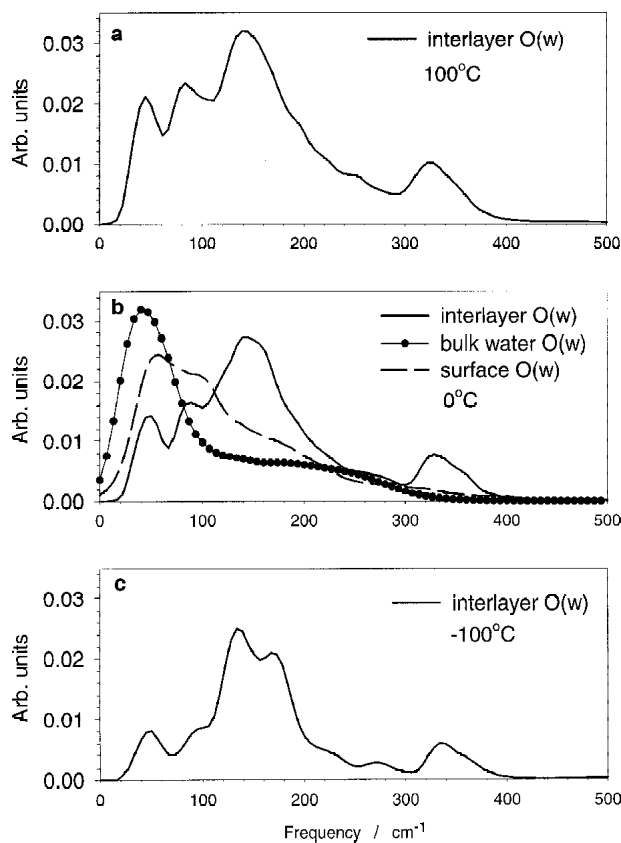


FIGURE 4. Spectral density of low frequency vibrational motions of water molecules in the interlayer.

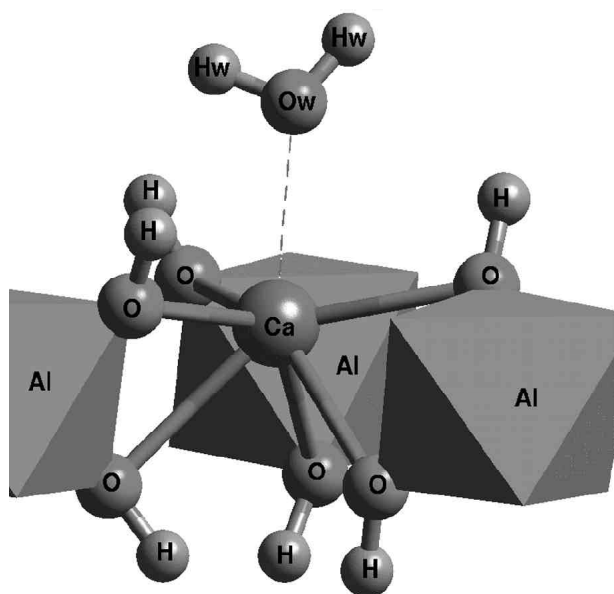


FIGURE 5. Sevenfold-coordinated environment of a Ca atom in the hydroxide layer and the Ca-OH<sub>2</sub> electrostatic bonding in hydrocalumite.

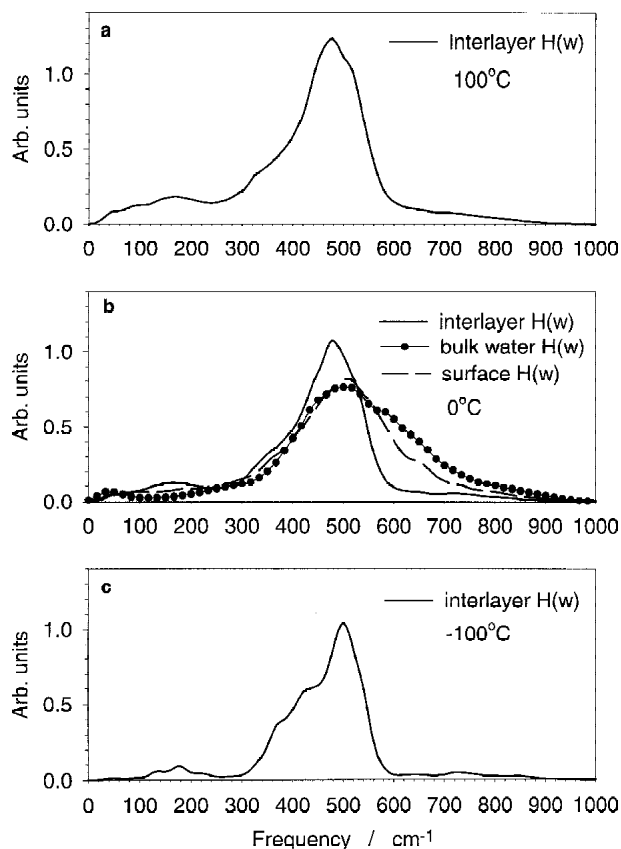


FIGURE 6. Spectral density of H<sub>2</sub>O molecular librations (hindered rotations) in the interlayer and on the surface of hydrocalumite.

TABLE 3. Calculated diffusion coefficients of interlayer and surface species (cm<sup>2</sup>/s)

	Cl <sup>-</sup>	H <sub>2</sub> O
Interlayer	$<< 10^{-7}$	$<< 10^{-7}$
Surface (inner sphere)	$8.1 \times 10^{-7}$	$5.0 \times 10^{-6}$
Surface (outer sphere)	$2.6 \times 10^{-6}$	$1.3 \times 10^{-5}$
Bulk NaCl solution	$1.1 \times 10^{-5}$	$1.8 \times 10^{-5}$

ferent hydrogen bonding environment in these two cases.

Although the general scheme for the interlayer water dynamics suggested by van der Pol et al. (1994) for hydrocalumite (Mg,Al MMLH with interlayer carbonate) based on <sup>1</sup>H NMR results is generally confirmed by computer simulations, our results show that the time-averaged direction of the C<sub>2</sub> symmetry axis of interlayer water molecules is neither preferably parallel (Marcelin et al. 1989), nor definitely perpendicular to the layers, but has some intermediate orientation. The calculated distribution of instantaneous dihedral angles formed between water molecular planes and the (001) crystallographic plane exhibits a distinct maximum at about 50 degrees.

Diffusion coefficients of Cl<sup>-</sup> anions and water molecules were calculated from mean square displacement of those species (Table 3). Statistical errors of these calculations are estimated to be roughly 10–15%. The results in Table 3 show that on the space and time scale of the simulations there is no statistically appreciable diffusion in the interlayer, which is ex-

perimentally known to be about  $10^{-8}$  cm<sup>2</sup>/s (e.g., Buenfeld and Zhang 1998). However, the simulations show two distinct types of surface Cl<sup>-</sup> with diffusion rates differing by a factor of ~3. One type is strongly bonded directly to the OH groups of the hydroxide layer (inner-sphere surface complexing) and strongly preferred (~85% of all surface chlorides present). The other type has one molecular layer of water between the anion and surface hydroxides (outer-sphere surface complexing), making them much more mobile (see Fig. 1). These results are in good qualitative agreement with the <sup>35</sup>Cl<sup>-</sup> NMR data for hydrocalumite under controlled relative humidity conditions. These observations show that at high humidity, when essentially bulk water is present, at least some of the surface Cl<sup>-</sup> undergo rapid isotropic averaging, as indicated by the narrow NMR peak (Kirkpatrick et al. 1999). However, even the diffusion rates of the outer-sphere Cl<sup>-</sup> are almost an order of magnitude less than that of Cl<sup>-</sup> in bulk aqueous solution. The exchange of Cl<sup>-</sup> between inner-sphere and outer-sphere environments is clearly observable on the 100 ps time scale of our simulations. However, for a detailed comparison to the NMR data a quantitative analysis of the exchange dynamics is necessary, which would require more extended simulations.

The mobility of water molecules in all cases is greater than that of the corresponding chloride (Table 3). Inner-sphere and outer-sphere water molecules were defined as roughly corresponding, respectively, to the first and second molecular layers adjacent to the surface hydroxide layer. The calculated self-diffusion coefficients for water on the hydrocalumite surface are in very good quantitative agreement with the results of recent molecular dynamics simulations of water in porous Vycor glass (Spohr et al. 1999), where the surface consists of disordered Si-O-H.

### ACKNOWLEDGMENTS

The research was supported by NSF grant EAR 95-26317 (R.J.K., P.I.) and the NSF Science and Technology Center for Advanced Cement-Based Materials. Additional funding was provided by the U.S. Department of Energy, Office of Basic Energy Sciences, Geosciences Research, under contract DE-AC04-94AL85000 with Sandia National Laboratories. The computations were performed using the Cerius<sup>2</sup>-3.8 software package from Molecular Simulations Inc.

### REFERENCES CITED

- Aicken, A.M., Bell, I.S., Coveney, P.V., and Jones, W. (1997) Simulation of layered double hydroxide intercalates. *Advanced Materials*, 9, 496–500.
- Allen, M.P. and Tildesley, D.J. (1987) *Computer Simulation of Liquids*, 385 p. Oxford University Press, New York.
- Berendsen, H.J.C., Postma, J.P.M., van Gunsteren, W.F., and Hermans, J. (1981) Interaction models for water in relation to protein hydration, In B. Pullman, Ed., *Intermolecular Forces*, p.331–342. Riedel, Dordrecht.
- Birnin-Yauri, U.A. and Glasser, F.P. (1998) Friedel's salt, [Ca<sub>2</sub>Al(OH)<sub>6</sub>](ClOH)<sub>2</sub>H<sub>2</sub>O: Its solid solutions and their role in chloride binding. *Cement and Concrete Research*, 28, 1713–1723.
- Buenfeld, N.R. and Zhang, J.-Z. (1998) Chloride diffusion through surface-treated mortar specimens. *Cement and Concrete Research*, 28, 665–674.
- Chang, F.R.C., Skipper, N.T., and Sposito, G. (1997) Monte Carlo and molecular dynamics simulations of interfacial structure in lithium-montmorillonite hydrates. *Langmuir*, 13, 2074–2082.
- Chirlian, L.E. and Francl, M.M. (1987) Atomic charges derived from electrostatic potentials: A detailed study. *Journal of Computational Chemistry*, 8, 894–905.
- Delley, B. (1990) An all-electron numerical method for solving the local density functional for polyatomic molecules. *Journal of Chemical Physics*, 92, 508–517.
- Delville, A. (1995) Monte Carlo simulations of surface hydration—An application to clay wetting. *Journal of Physical Chemistry*, 99, 2033–2037.
- Eisenberg, D. and Kautzmann, W. (1969) *The Structure and Properties of Water*, 296 p. Oxford, U.K.
- Fischer, R., Kuzel, H.-J., and Schellhorn, H. (1980) Hydrocalumit: Mischkristalle von "Friedelschem Salz" 3CaO·Al<sub>2</sub>O<sub>3</sub>·CaCl<sub>2</sub>·10H<sub>2</sub>O und Tetracalciumaluminat-hydrat 3CaO·Al<sub>2</sub>O<sub>3</sub>·Ca(OH)<sub>2</sub>·12H<sub>2</sub>O. *Neues Jahrbuch für Mineralogie Monatshefte*, 1980, 322–334.
- Hartzell, C.J., Cygan, R.T., and Nagy, K.L. (1998) Molecular modeling of the tributyl phosphate complex of europium nitrate in the clay hectorite. *Journal of Physical Chemistry B*, 102, 6722–6729.
- Heinzinger, K. (1990) Molecular dynamics simulation of aqueous systems, In C.R.A. Catlow, Ed., *Computer modeling of fluids, polymers and solids*, p. 357–394. Kluwer Academic Publishing, Dordrecht.
- Kalinichev, A.G. and Heinzinger, K. (1992) Computer simulations of aqueous fluids at high temperatures and pressures. *Advances in Physical Geochemistry*, 10, 1–59.
- Karaborni, S., Smit, B., Heidug, W., Urai, J., and Vanoort, E. (1996) The swelling of clays—Molecular simulations of the hydration of montmorillonite. *Science*, 271, 1102–1104.
- Kirkpatrick, R.J., Yu, P., Hou, X., and Kim, Y. (1999) Interlayer structure, anion dynamics, and phase transitions in mixed-metal layered hydroxides: Variable temperature <sup>35</sup>Cl NMR spectroscopy of hydrocalumite and Ca-aluminate hydrate (hydrocalumite). *American Mineralogist*, 84, 1186–1190.
- Marcelin, G., Stockhausen, N.J., Post, J.F.M., and Schutz, A. (1989) Dynamics and ordering of interlayered water in layered metal hydroxides. *Journal of Physical Chemistry*, 93, 4646–4650.
- Molecular Simulations Inc. (1998) *Cerius<sup>2</sup>-3.8 User Guide*. Forcefield-Based Simulations, Inc., San Diego.
- Newman, S.P. and Jones, W. (1998) Synthesis, characterization and applications of layered double hydroxides containing organic guests. *New Journal of Chemistry*, 22, 105–115.
- Newman, S.P., Williams, S.J., Coveney, P.V., and Jones, W. (1998) Interlayer arrangement of hydrated MgAl layered double hydroxides containing guest terephthalate anions. *Journal of Physical Chemistry B*, 102, 6710–6719.
- Parrinello, M. and Rahman, A. (1981) Polymorphic transitions in single crystals: A new molecular dynamics method. *Journal of Applied Physics*, 52, 7182–7190.
- Passaglia, E. and Sacerdoti, M. (1988) Hydrocalumite from Monalto di Castro, Viterbo, Italy. *Neues Jahrbuch für Mineralogie Monatshefte*, 1988, 454–461.
- Perdue, J.P. (1991) Generalized gradient approximations for exchange and correlation: A look backward and forward. *Physica B*, 172, 1–6.
- Rustad, J.R., Wasserman, E., Felmy, A.R., and Wilke, C. (1998) Molecular dynamics of proton binding to silica surfaces. *Journal of Colloid and Interface Science*, 198, 119–129.
- Sacerdoti, M. and Passaglia, E. (1988) Hydrocalumite from Latium, Italy: its crystal structure and relationship with related synthetic phases. *Neues Jahrbuch für Mineralogie Monatshefte*, 1988, 462–475.
- Schmassmann, A., Tarnawski, A., Flogerzi, B., Sanner, M., Varga, L., and Halter, F. (1993) Dynamics of drug interference with healing of experimental gastric ulcers. *European Journal of Gastroenterology and Hepatology*, 5, S13–S20.
- Smith, D.E. (1998) Molecular computer simulations of the swelling properties and interlayer structure of cesium montmorillonite. *Langmuir*, 14, 5959–5967.
- Spohr, E., Hartnig, C., Gallo, P., and Rovere, M. (1999) Water in porous glasses. A computer simulation study. *Journal of Molecular Liquids*, 80, 165–178.
- Taylor, H.F.W. (1997) *Cement Chemistry*, 2<sup>nd</sup> ed. Thomas Telford Publishing, London.
- Teleman, O., Jönsson, B., and Engström, S. (1987) A molecular dynamics simulation of a water model with intramolecular degrees of freedom. *Molecular Physics*, 60, 193–203.
- Teppen, B.J., Rasmussen, K., Bertsch, P.M., Miller, D.M., and Schafer, L. (1997) Molecular dynamics modeling of clay minerals 1. Gibbsite, kaolinite, pyrophyllite, and beidellite. *Journal of Physical Chemistry B*, 101, 1579–1587.
- Terzis, A., Filippakis, S., Kuzel, H.-J., and Burzlaff, H. (1987) The crystal structure of Ca<sub>2</sub>Al(OH)<sub>6</sub>Cl·2H<sub>2</sub>O. *Zeitschrift für Kristallographie*, 181, 29–34.
- Ulibarri, M.A., Pavlovic, I., Hermosin, M.C., and Comejo, J. (1995) Hydrocalumite-like compounds as potential sorbents of phenols from water. *Applied Clay Science*, 10, 131–145.
- van der Pol, A., Mojte, B. L., van de Ven, E., and de Boer, E. (1994) Ordering of intercalated water and carbonate anions in hydrocalumite. An NMR study. *Journal of Physical Chemistry*, 98, 4050–4054.
- Williams, S.J., Coveney, P.V., and Jones, W. (1999) Molecular dynamics simulations of the swelling of terephthalate containing anionic clays. *Molecular Simulation*, 21, 183–189.
- Woods, R.J., Khalil, M., Pell, W., Moffat, S.H., and Smith, V.H. Jr. (1990) Derivation of net atomic charges from electrostatic potentials. *Journal of Computational Chemistry*, 11, 297–310.

MANUSCRIPT RECEIVED SEPTEMBER 7, 1999

MANUSCRIPT ACCEPTED FEBRUARY 17, 2000

PAPER HANDLED BY BJOERN WINKLER